Silicon (2023) 15:739–753
https://doi.org/10.1007/s12633-022-02037-3

ORIGINAL PAPER

Investigation on Thermophysical and Physicochemical Properties of CaO-SiO_2-CaF_2-22.5%TiO_2 Silica Based Electrode Coating System

Vijay Kumar[1] · **Rahul Chhibber**[1] · **Lochan Sharma**[2]

Received: 27 April 2022 / Accepted: 22 July 2022 / Published online: 3 August 2022

Abstract
The present paper aims to study the thermophysical and physicochemical properties of CaO-CaF_2-SiO_2-22.5% TiO_2 based electrode coating for welding the components of advanced ultra-supercritical power plants. The mixture design methodology was used to formulate thirteen coating mixtures to explore the effect of flux coating properties, i.e., density, change in enthalpy, weight loss, thermal conductivity, specific heat, and thermal diffusivity. Flux coating properties play an essential role in achieving better weldments. Fourier transformation and X-ray diffraction were used to analyze electrode coating composition structural behavior. The coating composition was also characterized by using a thermogravimetric analyzer and hot disc apparatus, and after that, a regression model analysis was carried out to study individual, and their interaction effects on the thermophysical and physicochemical properties. CaO.CaF_2, CaO.SiO_2, and CaF_2.SiO_2 is the most effective binary mixture which has an increasing effect on density. The weight loss of coating observed during thermogravimetric analysis is affected by individual constituents significantly. The binary interaction of SiO_2.CaO and CaF_2.SiO_2 is the most favorable and has an increasing effect on weight loss. Individual components affect change in enthalpy significantly. The binary interaction of CaO.SiO_2 and CaF_2.SiO_2 is the most effective and has an increasing effect on change in enthalpy. The thermal properties of coating composition observed during hot disc are affected by individual and binary mixture constituents. Binary mixture CaF_2.CaO and CaF_2.SiO_2 is having an increasing effect on thermal conductivity. Binary mixture SiO_2.CaO shows a decreasing impact on thermal diffusivity. Binary mixture constituents CaF_2.CaO, SiO_2.CaO is the most effective and has an increasing effect on specific heat.

Keywords Mixture design · Power plant · Coatings · Thermophysical · Regression · Physicochemical

1 Introduction

In the present situation of power generation, advanced ultra-supercritical thermal power plants have gained considerable interest because of their environmental friendliness and higher efficiency by increasing the working pressure and temperature. High temperature, pressure, and corrosive environments make fabricating advanced ultra-supercritical power plant components difficult [1]. In the AUSC power plant, different parts work at distinct temperature ranges. Therefore suitable materials are required to fulfil the desired operating conditions. Various dissimilar welds are there in a power plant. Dissimilar welds, a nickel-based alloy, work at higher temperature regions, and austenitic stainless steels operate at moderate temperature regions because high-temperature creep and corrosion resistance are of prime interest. Failures occur in dissimilar welds due to various reasons such as the difference in the thermal coefficient expansion, unmixed zone, welding parameters, hot cracking, carbon migration, etc. Due to the formation of different zones such as Heat-affected zone (HAZ), partially melted zones (PMZ), and unmixed zones affect the microstructural and mechanical properties of dissimilar welds [2–6].

One of the factors involved in dissimilar metal joints is selecting the welding process, parameters, and coating

✉ Vijay Kumar
vijay.4@iitj.ac.in

Rahul Chhibber
rahul_chhibber@iitj.ac.in

Lochan Sharma
lochan.e9455@cumail.in

[1] Mechanical Engineering Department, Indian Institute of Technology Jodhpur, Jodhpur, India

[2] University Center for Research & Development, Chandigarh University, Mohali, Punjab 140413, India

constituents. In the SMAW process, flux-coated electrodes carry out different functions to achieve better weld performance, such as arc stability and slag detachability and produce slag to protect the weld pool from the environment, geometry, and quality bead shape. The different fluxes (acidic, basic, neutral) can be used to make an electrode coating, which influences slags' thermophysical properties. Electrode coating formulation has an essential role in the mechanical, weld metal chemistry, and microstructural properties of weldments [7–9]. A slag metal reaction occurs when the coating composition's ingredients are mixed with the molten weld pool during the welding process. The various properties of thermophysical and physicochemical coatings influence the behavior of weld deposits. The weld metal pool's fluidity decreases with a highly viscous flux coating composition, and highly negative enthalpy adversely affects the weld metal and heat-affected zone [10–12]. Various researchers have studied the effects of fluxes and coating composition ingredients and their chemistry on weld metal's mechanical performance [13–16]. The electrode coating releases gases that shield the weld pool from the environment and maintain arc stability. CaO addition decreases the weld hydrogen content, and an increase in basicity index was observed. A significant decrease in viscosity and improvement of arc stability was observed with the addition of optimum content of CaO in the weld region. Slag detachability, as well as density, has been significantly improved with the addition of CaF_2. The flow rate of molten metal and excess hydrogen content in the weld region has also considerably improved with the addition of CaF_2 in the coating mixture. The addition of both SiO_2 and TiO_2 in the coating mixture helps in enhancing the slag detachability and enhances the surface finish of weld metal. Higher basicity flux lower the weld pool's oxygen content, which is also the primary concern for weld performance. Previous researchers also studied the effect of parameters on microstructure of composite electrode and response surface methodology [17–27]. The availability of literature is limited in the open domain on the fluxes and coating composition's thermophysical and physicochemical properties [28–31]. The present paper examines the Physico-chemical and thermophysical properties of CaO-CaF_2-SiO_2-22.5% TiO_2 based electrode coating for the AUSC power plant. Experiments were conducted using the vertices design method. Thirteen sets of electrode coating compositions have been formulated. The electrode coating composition was crushed into powder form to determine properties like density, enthalpy change, specific heat, thermal conductivity, thermal diffusivity, and weight loss. X-ray diffraction and FTIR were used to analyze electrode coating composition structural behavior. The coating composition was characterized by using a thermogravimetric analyzer and hot disc apparatus.

2 Materials

The minerals used to prepare electrode coating are calcite, fluorspar, silica and rutile. High basicity index electrodes are desirable for high-temperature applications because of low hydrogen. Using the XRF technique, the chemical composition of minerals was obtained, which is represented in Table 1.

3 Design of Experiment

Extreme vertices methodology given by Mclean and co-authors [32] was adapted to design coating mixtures. The lower as well as upper limit for the constraint mixture of 'n' components were given in the developed design matrix as per Eqs (1 and 2).

$$0 \le a_i \le y_i \le b_i \le 100 \tag{1}$$

$$\sum_{i=1}^{m} yi = 100 \tag{2}$$

Figure 1 indicates CaO-SiO_2-CaF_2, a ternary diagram that was used to indicate the points corresponding to lowest melting points and their corresponding design space.

In this study overall composite melting temperature of coating decides the percentage composition of individual coating components. Because the overall composite melting temperature of coating should be lower than that of base metal. The ternary diagram encircled points represents the percentage composition selection region as well as overall composite melting temperature of slag [7–9]. The lower and higher limits of flux compositions were scaled to a total of 75%, and the remaining 22.5% rutile was added to get better slag detachability, and 2.5% other coating constituents were mixed. Range of different coating constituents were shown by eq. 3 and 4. In SMAW process, electrode coating should melt first, then filler wire and base metal should remain the same in the molten state after weld metal solidifies; while deciding the temperature of the composite melting point of

Table 1 Chemical composition

Element (Wt%)	Calcite	Silica	Fluorspar	Rutile
Aluminium	4.16	2.79	4.99	5.97
Silicon	2.89	97.16	1.40	5.04
Calcium	81.45	0.48	92.77	–
Titanium	–	–	–	87.46
Iron	0.74	0.17	0.41	1.57
Magnesium	9.48	–	–	–
Sulphur	–	0.29	–	0.29

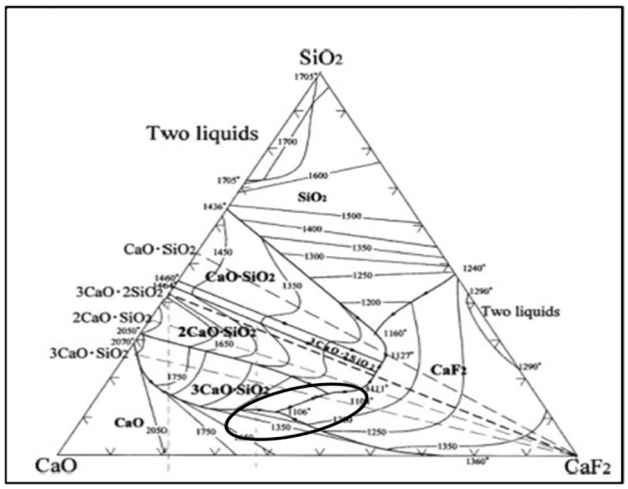

Fig. 1 Experimental diagram of the CaO- SiO_2-CaF_2 flux system [33]

coating composition; this aspect was considered so that it remains under limits.

$$\begin{aligned} 30 \le \mathrm{CaO} \le 35 \\ 25 \le \mathrm{CaF_2} \le 30 \\ 10 \le \mathrm{SiO_2} \le 15 \end{aligned} \tag{3}$$

$$\sum_{i=1}^{3} xi = 75 \tag{4}$$

Table 2 represents the design matrix for 13 coating mixtures and Fig. 2 shows the design space diagram for 13 coating mixtures.

Table 2 Design matrix of 13 coating compositions

Coating Number	Composition of Mixture			Basicity Index
	CaO	CaF_2	SiO_2	
1	35.00	25.00	15.00	2.29
2	32.50	30.00	12.50	2.63
3	34.17	12.92	27.92	2.57
4	32.92	29.17	12.92	2.57
5	35.00	27.50	12.50	2.63
6	31.67	29.17	14.17	2.39
7	34.17	29.17	11.67	2.76
8	32.92	27.92	14.17	2.39
9	30.00	30.00	15.00	2.29
10	32.50	27.50	15.00	2.29
11	34.17	26.67	14.17	2.39
12	35.00	30.00	10.00	3.06
13	33.33	28.33	13.33	2.51

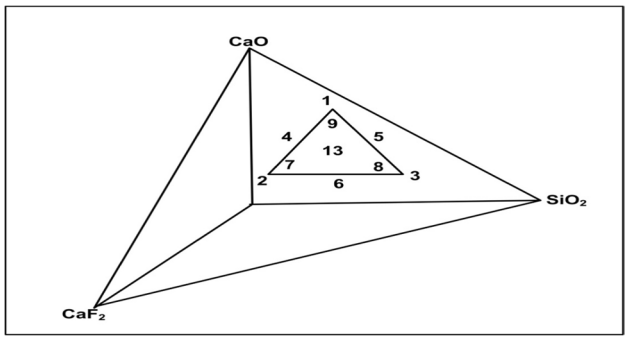

Fig. 2 Design space diagram

4 Experimentation

As per the design matrix coating composition, the individual mineral powder was weighed by the digital weighing balance and mixed with the help of a dry mixer. After the powder mixing,

potassium silicate acts as a binder added to the mixture to prepare the wet mixture and then left for 35 minutes in the mixer to get properly mixed. By lab-scale extruder, Inconel 617 core wire was extruded by wet mixture to obtain electrodes and then air-dried the electrodes for 36 hours and then baked in the oven for 3 hours at 150° C. The fully dry coating was removed from the electrodes, crushed to the small size of approximately 260 µm, and mixed adequately in muller to perform further various characterizations. FTIR and XRD techniques were used to characterize the coating specimen's structural behavior. Different phases present were analyzed by the monochromatic Cu Kα radiation x-ray diffraction technique. To determine various bond lengths and bonds in the composition FTIR technique was used with a resolution of 2 cm^{-1} in the range of wave number 400-4000 cm^{-1}. The coating powder's bulk density was measured by weighing the amount of flux powder using 10 mL volume in a measuring cylindrical flask. Thermogravimetric analyzer (TGA) measured change in enthalpy and weight loss by the coating sample heating from temperature 30 °C to 900 °C at the constant heating of 20 °C/min. Thermal characterization of coatings such as thermal conductivity, specific heat, and thermal diffusivity was done by hot disc technique using a Kapton sensor size of 3.415 mm. A descriptive figure (Fig. 3) shows a detailed schematic diagram for the experimental process.

5 Results

For density measurements, the standard procedures to find the bulk density of powder specimens were used. Density measurement was performed thrice for each coating

Fig. 3 Schematic diagram for experimentation

composition and reported the average density value. The coating C1 was recorded as a minimum density of 1.539 g/cm^{3,} whereas a maximum density of 1.693 g/cm^3 was reported for coating C6. Equation 5 shows the formula to find the density. Table 3 shows the quantitative values for 13 coating mixtures.

$$\rho = \frac{Mass}{Volume} \tag{5}$$

Whereas ρ is density (g/cm^3), V is the volume displaced from 10 cm^3 for each specimen. Weight of flux powder measured in grams is term as m, Fig. 4 represents the average density variation of all samples.

To analyse the thermal behaviour of 13 coating mixtures, a hot disk technique was utilized and their quantitative values were given in Table 4. C1 coating gives the minimum value of thermal conductivity (0.2085 W/mK), while C5 coating shows a maximum value (0.2592 W/mK). The maximum value of thermal diffusivity (0.2587mm^2/s) was observed for C5 coating, while C3 coating gives a higher

Table 3 Density Measurement of Coating

Coating Number	Density in (gram/cm^3)
C-1	1.539
C-2	1.686
C-3	1.672
C-4	1.673
C-5	1.668
C-6	1.695
C-7	1.693
C-8	1.671
C-9	1.593
C-10	1.671
C-11	1.686
C-12	1.669
C-13	1.667

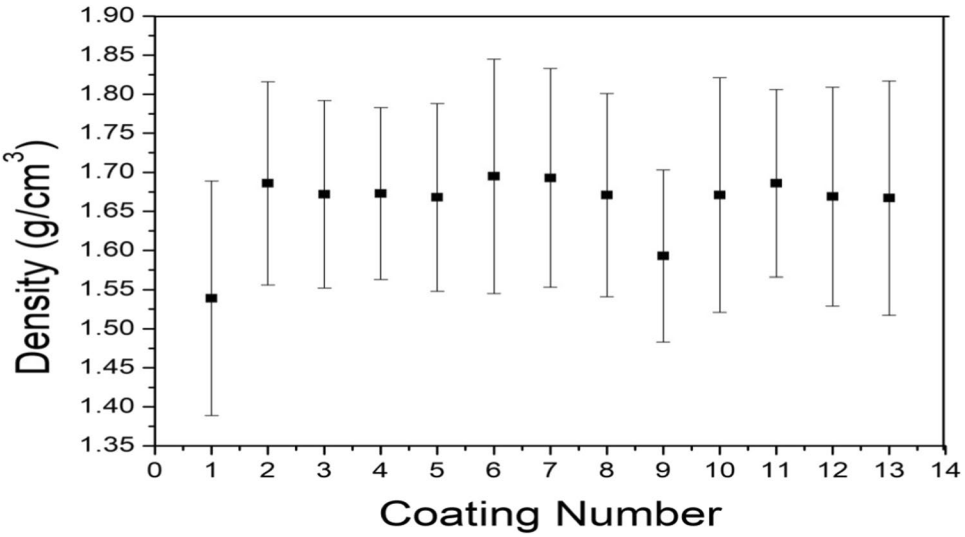

Fig. 4 Variation of density for various coatings

Table 4 Thermal analysis of different flux coating composition

Coating Number	Thermal conductivity (W/mK)	Thermal diffusivity (mm^2/s)	Specific heat (M.J./m^3K)
C-1	0.2085	0.2440	0.9368
C-2	0.2328	0.2117	1.100
C-3	0.2508	0.2233	1.123
C-4	0.2502	0.2334	1.072
C-5	0.2592	0.2587	1.002
C-6	0.2308	0.2120	1.089
C-7	0.2527	0.2420	1.045
C-8	0.2293	0.2203	1.041
C-9	0.2128	0.2004	0.9002
C-10	0.2564	0.2312	1.109
C-11	0.2576	0.2348	1.097
C-12	0.2557	0.2388	1.071
C-13	0.2493	0.2320	1.074

value of specific heat (1.123 MJ/m^3K) as compared to the remaining coating mixtures. To find out the thermal conductivity of 13 coating mixtures, eq. 6 was used.

$$K = \frac{QL}{A\Delta T} \tag{6}$$

Whereas K is thermal conductivity (W/mK), A is the surface contact area (m^2), Q is the amount of heat transfer through flux measured (W). Temperature differenceΔT is measured (Kelvin). To find the thermal diffusivity, eq. 7 was used.

$$\alpha = \frac{K}{\rho Cp} \tag{7}$$

K is thermal conductivity (W/mK), specific heat capacity Cp in (J/kg K), and density ρ in (kg/m^3). Amount of heat absorbed or released by the coating specimen is used to find its specific heat (C) which is given by eq. 8.

$$c = \frac{Q}{mdT} \tag{8}$$

A thermogravimetric analyzer was used to estimate the variation in enthalpy and thermal stability of 13 coating mixtures. Weight changes of coating sample measured with the function of temperature and time. Initially, the coating powder was heated to 30 °C from room temperature, and then confined for one minute. Then, the powder sample was heated at a rate of 20 °C per minute from 30 °C to 900^0Cin a controlled environment. Table 5 shows the weight change behavior of different coating samples. It is always desired to have a more thermally stable coating mixture for high-temperature applications. With a weight change of 13.70%, the C9 coating composition is thermally more stable, while the C12 coating composition is lesser stable, with a maximum weight change of 15.96% because weight loss at higher temperatures is related to the thermal stability of the coating constituents. An increase in the CaO content in the coating mixture influences the weight loss due to its hygroscopic nature. Moisture has significant effects on the coating mixture containing basic oxide. A higher amount of CaO results in higher weight loss [8]. Figure 5 shows change in weight loss corresponding to the temperature.

The thermogravimetric analysis also provides the value of change in enthalpy associated with the coating sample's heating. Enthalpy represents total heat related to the process and the quantity of work done by the system or to the system. Hence, the negative enthalpy value indicates that the system does work, which implies that heat is released

Table 5 Thermogravimetric analysis for weight loss

Coating Number	Starting Weight (W_i)	Final Weight (W_f)	Weight change ($\Delta W = W_i - W_f$)	Change in weight(% ΔW)
1	13.778	11.585	2.193	15.91
2	14.200	12.117	2.083	14.66
3	13.991	11.802	2.189	15.64
4	11.294	9.605	1.689	14.95
5	13.977	11.759	2.218	15.86
6	13.736	11.701	2.035	14.81
7	11.932	10.051	1.881	15.76
8	12.363	10.379	1.984	16.04
9	14.436	12.454	1.982	13.70
10	12.956	11.005	1.951	15.05
11	13.021	10.998	2.023	15.53
12	11.260	9.462	1.798	15.96
13	11.623	9.770	1.853	15.94

during the process. The nature of the process is exothermic, whereas the enthalpy's positive value indicates work is done on the system, which implies that heat is absorbed during the process. The nature of the process is endothermic. In the welding process, the heating of the electrode coating releases heat, which should not be too high; this leads to an unfavourable effect on the heat-affected zone and welded zone. Table 6 represents the quantitative value of the change in enthalpy for 13 coating mixtures. The minimum value of enthalpy change (18,484.10 J/g) was observed in a C3 coating, while maximum enthalpy change (32,274.60 J/g) was noticed in a C12 coating. Relations between heat flow and temperature for different coatings are shown in Fig. 6. The area determines an enthalpy value under the curve method.

XRD and FTIR were performed to analyze the structural behavior of all coating compositions. Figure 7 shows various peaks that indicate the different phases present in the flux coating composition. FTIR analysis was performed at the range of wave number 400 - 4000 cm $^{-1}$ with resolution ±2 cm $^{-1}$. FTIR analysis reveals the information regarding the presence of various bond lengths. Due to the same coating constituents, a similar FTIR pattern was observed for all coating. Variation in peak intensity is due to the difference in composition. Available literature reveals the formation of various types of bonds in the same peak ranges [34–37]. The Titanyl group (Ti-O) symmetric stretching was observed at the peak region of 700-750 cm^{-1}, and Si-OH stretching vibrations were observed at 750-800 cm^{-1}. Si-O asymmetric vibration mode was seen in the region of 1000-1250 cm^{-1}. Due to the complex SiO_4 ion formation, the Si-O Anti symmetric vibration mode was observed in the peak region of 1250-1500 cm^{-1}. The OH vibration mode and H-OH bonding were seen in the narrow region of peaks 1500-1750 cm^{-1} and 3250-3500 cm^{-1}. Figure 8 represents the FTIR curve for the coating mixture.

6 Development of the Regression Model

Design-Expert statistical software tools are used to develop the regression equations for the coating properties [7–9]. The effect of individual coating and their component interaction on the mixture using the obtained results were studied and shown by Eqs. 9-14.

$$\begin{aligned}\text{Density}\left(g/cm^3\right) = {} & -0.22794 \text{ x CaO} - 0.32734 \text{ x } CaF_2 \\ & -0.15872 \text{ x } SiO_2 + 0.015503\text{x CaO x } CaF_2 \\ & +6.36752 \text{ x}10^{-3} \text{ x CaO x } SiO_2 \\ & +8.49155 \text{ x } 10^{-3} \text{ x } CaF_2 \text{ x } SiO_2\end{aligned} \tag{9}$$

$$\begin{aligned}\text{Enthalpy (J/g)} = {} & +9525.51090 \text{ x CaO} + 10092.30857 \text{ x}CaF_2 \\ & -44460.64911 \text{ x } SiO_2 - 652.78729 \text{ x CaO x } CaF_2 \\ & +625.82508 \text{ x CaO x } SiO_2 + 810.11224 \text{ x } CaF_2 \text{ x } SiO_2\end{aligned} \tag{10}$$

$$\begin{aligned}\text{Thermal Conductivity} \\ \text{(W/mK)} = {} & -0.055983 \text{ x CaO} - 0.14877 \text{ x } CaF_2 \\ & +7.53252 \text{ x } 10^{-3} \text{ x } SiO_2 + 5.51114 \text{ x } 10^{-3} \text{ x CaO x } CaF_2 \\ & -7.43835 \text{ x } 10^{-4}\text{x CaO x } SiO_2 + 3.59173 \text{ x } 10^{-3} \text{ x } CaF_2 \text{ x } SiO_2\end{aligned} \tag{11}$$

$$\begin{aligned}\text{Thermal Diffusivity} \\ \left(mm^2/s\right) = {} & +0.018508 \text{ x CaO} - 0.025606 \text{ x } CaF_2 \\ & +3.45453 \text{ x } 10^{-3} \text{ x } SiO_2 + 3.07653 \text{ x } 10^{-4}\text{x CaO x } CaF_2 \\ & -1.04708 \text{ x } 10^{-3} \text{ x CaO x } SiO_2 + 1.23687 \text{ x } 10^{-3}\text{x } CaF_2 \text{ x } SiO_2\end{aligned} \tag{12}$$

$$\begin{aligned}\text{Specific Heat}\left(MJ/m^3K\right) = {} & -0.52171 \text{ x CaO} - 0.46352 \text{ x } CaF_2 \\ & -0.083615 \text{ x } SiO_2 + 0.027043 \text{ x CaO x } CaF_2 \\ & +0.014943 \text{ x CaO x } SiO_2 \text{ x} + 1.45775 \text{ x } 10^{-3} \text{ x } CaF_2 \text{ x } SiO_2\end{aligned} \tag{13}$$

$$\begin{aligned}\text{Weight Loss (mg)} = {} & +0.77415 \text{ x CaO} + 1.06742 \text{ x } CaF_2 \\ & -1.07067 \text{ x } SiO_2 - 0.049928 \text{ x CaO x } CaF_2 \\ & +0.012484 \text{ x CaO x } SiO_2 + 4.80055 \text{ x } 10^{-3} \text{ x } CaF_2 \text{ x } SiO_2\end{aligned} \tag{14}$$

The variance of adequacy was checked by the F test using the above-developed regression models. By using backward and forward techniques of ANOVA, all the regression models were developed. ANOVA is used to investigate the effect of interactions between mineral ingredients on the results obtained. Depending on the influence on the acquired output, it was divided into two categories: significant and increasing impacts and non-significant and decreasing effects. Primary, binary, and ternary mixtures with a p value less than 0.05 are statistically significant, and those with a p value more than 0.05 are not significant. Table 7 represents the results

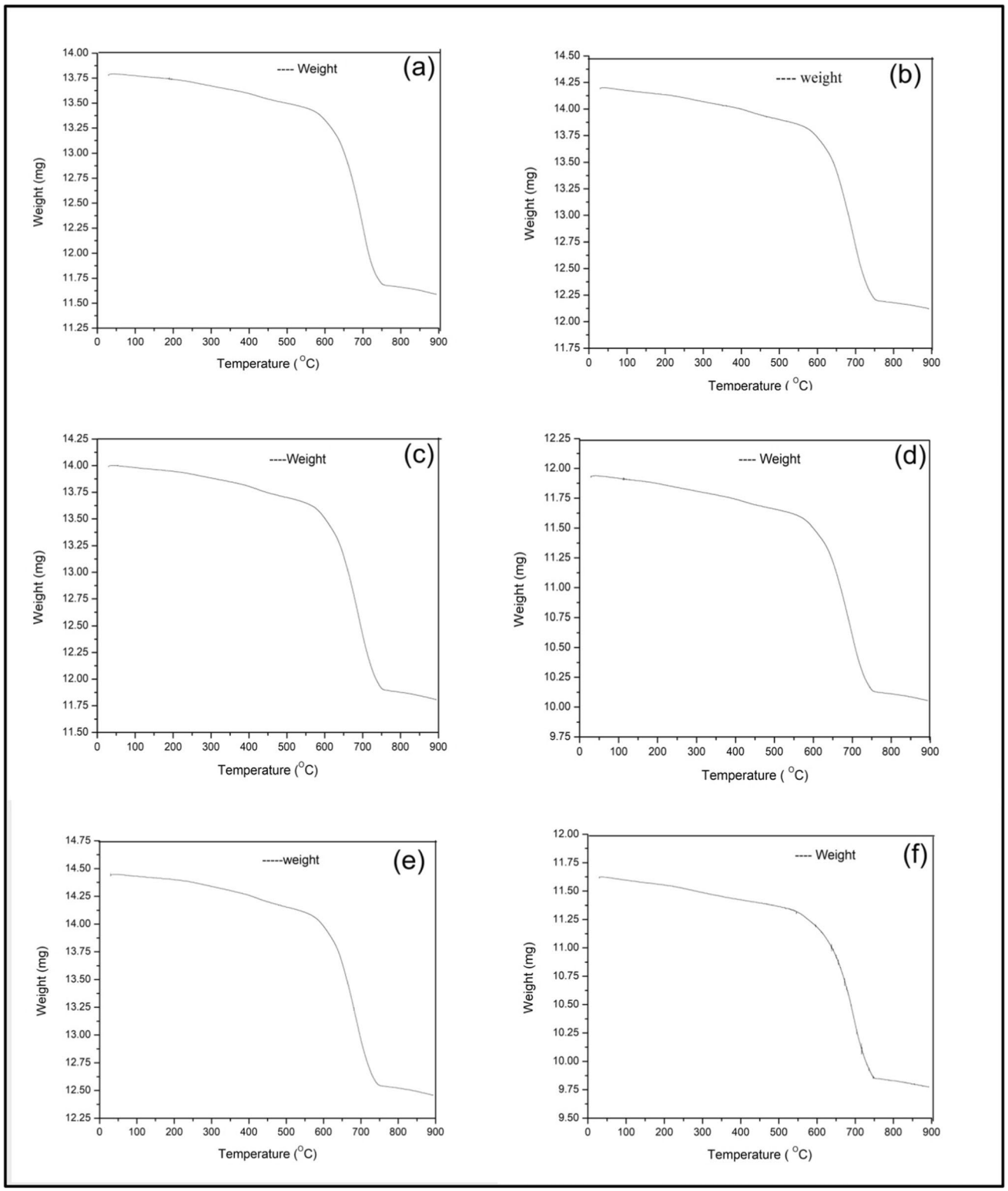

Fig. 5 Weight Loss for various coating composition: (**a**) C-1, (**b**) C-2, (**c**) C-3, (**d**) C-7 (**e**) C-9, (**f**) C-12

of ANOVA. The interaction influence of primary and binary coating mixture on the different thermophysical responses is shown in Table 8.

Figure 9 (a-f) shows the plot between each response's predicted and actual value, which indicates a closeness to the response.

Table 6 Enthalpy values

S. No	Coating Number	Heating Rate (°C./min)	Enthalpy Change (ΔH in J/g)
1	C-1	20	−20,339.60
2	C-2	20	−21,140.10
3	C-3	20	−18,484.10
4	C-4	20	−23,506.20
5	C-5	20	−22,065.60
6	C-6	20	−20,353.40
7	C-7	20	−23,162.20
8	C-8	20	−26,387.00
9	C-9	20	−19,829.20
10	C-10	20	−22,138.60
11	C-11	20	−20,192.10
12	C-12	20	−32,274.60
13	C-13	20	−22,129.90

Thermophysical and physicochemical properties are significantly affected by flux coating constituents. In the welding process, the flux coatings are revealed to high temperatures, and due to this, several chemical reactions occur. To get better weld mechanical properties, it is essential to select suitable electrode coatings. Different regression models in terms of various thermophysical responses were developed. From the density model it reported that individual constituents affect density significantly. $CaO.CaF_2$, $CaO.SiO_2$, and $CaF_2.SiO_2$ is the most effective binary mixture which has an increasing effect on density. The lower value (CV = 1.34%) of the variance coefficient shows the experimentation's precise and good reliability. The developed model was checked by quadratic regression and had a 0.0078 p value, which shows significant and acceptable under confidence limits of 95%. During the welding process, the slag metal reaction takes place with coated electrodes. If an oxide inclusion increases, it will decrease the fluidity and increase density due to the network former. Silicon dioxide is known as a chain network former. SiO_2 and CaO present in the coating, and due to chemical reaction, $SiO_2 + 2O^{2-} = SiO_4{}^{4-}$; $CaO = Ca^{2+} + O^{2-}$, to form $SiO_4{}^{4-}$ complex silicate ion. A significant increase in density has been reported in the literature due to the involvement of these silicate ions. Several weld defects can arise if the density has high fluidity. In welding, the thermal stability of flux coating is essential at high temperatures. Due to the thermal instability of coating, weld quality may be affected adversely. A thermogravimetric analyzer was used to measure the coating's thermal stability as heating in the controlled environment to calculate the enthalpy change and weight loss. The regression model for weight loss is significant, having a p value of 0.0306. It reported that binary interaction of $SiO_2.CaO$ and $CaF_2.SiO_2$ is the most favorable and has an increasing effect on weight loss. The coating mixture C9 is thermally more stable with least weight loss, and coating mixture C12 is less stable with more weight loss because weight loss at higher temperatures is related to the thermal stability of the coating constituents. An increase in the CaO content in the coating mixture influences the weight loss due to its hygroscopic nature. The hygroscopic nature leads to the decrease in viscosity of the slag and increases the chances of contamination from air or moisture. Moisture has significant effects on the coating mixture containing basic oxide. A higher amount of CaO results in higher weight loss [8]. The lower value of the variance coefficient (CV = 4.92%) shows better reliability and precision. The developed regression model for enthalpy represents a significant p value of 0.0425, and it was observed that binary interaction of $CaO.SiO_2$ and $CaF_2.SiO_2$ is the most effective and has an increasing effect on change in enthalpy, while other components show opposite effect on change in enthalpy. Heat evolved due to chemical reaction occurs during the welding process is called enthalpy. In the present study, experimental results of change in enthalpy give the negative value, which reveals that the exothermic chemical reactions take place. It should not be either too high or too low. The lower value (CV = 10.33%) of the coefficient of variance shows precise and better reliability. A hot disc experiment was used to measure the coating's thermal property, i.e., thermal conductivity, specific heat, and diffusivity which is significantly dependent on coating composition. The thermal behavior of coatings affect significantly by the presence of the network former. Due to the formation of covalently bonded Si^{4+} ions in the silica network chain, the thermal conductivity of electrode coating increases which contains higher SiO_2 content [38]. The regression model for thermal conductivity gives a p value of 0.0248, which is under the acceptable limit. The thermal properties of coating composition observed during hot disc are affected by individual and binary mixture constituents. Binary mixture $CaF_2.CaO$ and $CaF_2.SiO_2$ is having an increasing effect on thermal conductivity while other components show negative effect on thermal conductivity. For the model of thermal conductivity, 4.28% variance coefficient was observed, which is least than the other properties and indicates better reliability and precision in the experimental. Similarly, the developed regression model for thermal diffusivity with a p value of 0.0260 indicates significant and it states that primary constituents affect the thermal diffusivity significantly. Binary mixture $CaF_2.CaO$, $CaF_2.SiO_2$ shows an increasing effect on thermal diffusivity. A lower variance coefficient (4.12%) was shown with this model, indicating good precision and reliability for experimentation. Specific heat should be neither too high nor too low during the welding process as it affects the weld quality. The developed model for specific heat having a p value of 0.0332 is significant. Binary mixture

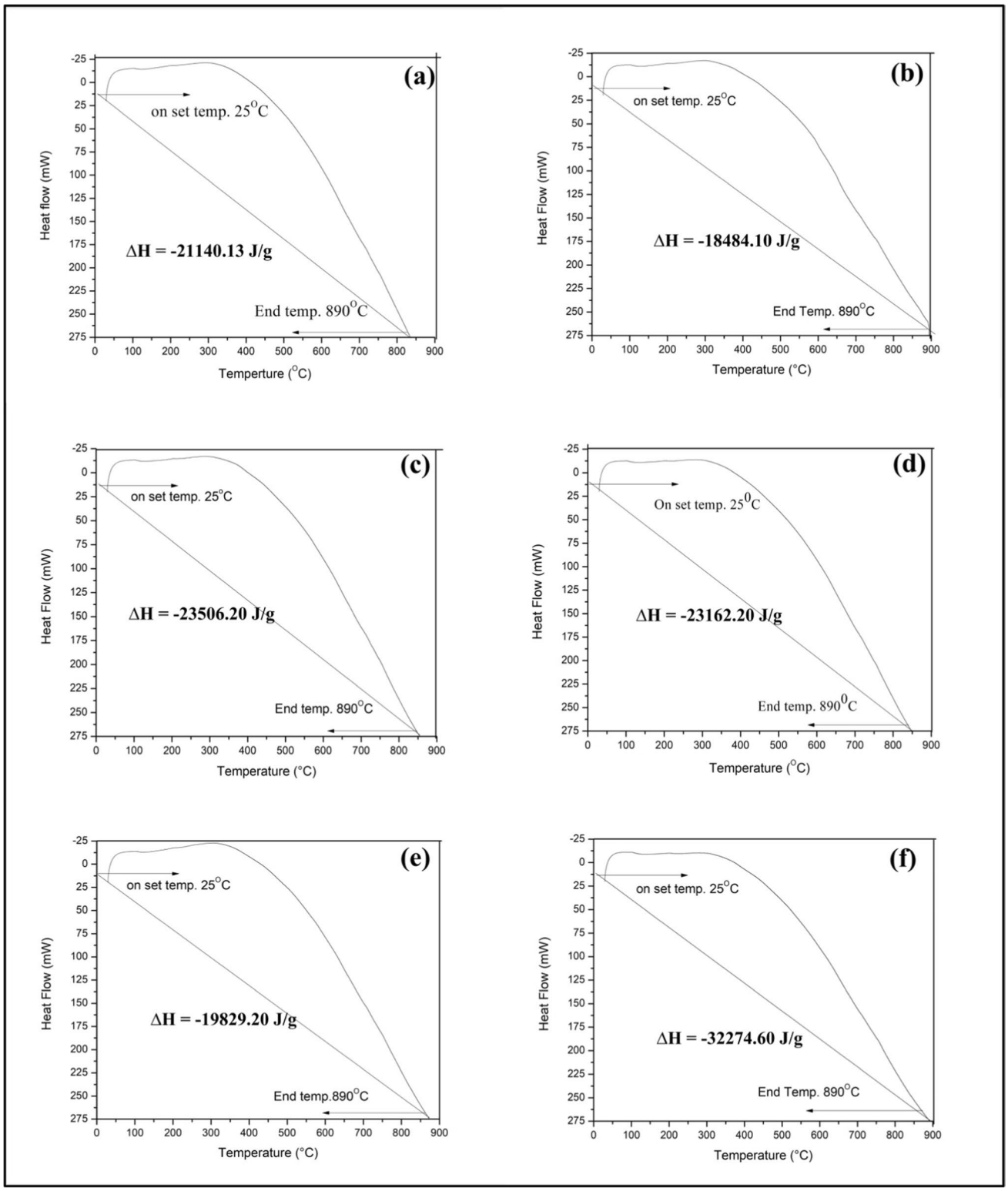

Fig. 6 Heat flow of various flux coating: (**a**) C-2, (**b**) C-3, (**c**) C-4, (**d**) C-7, (**e**) C-9, (**f**) C-13

constituents CaF_2.CaO, SiO_2.CaO is the most effective and has an increasing effect on specific heat. A lower C.V value of 4.01% was observed with this model, which describes good precision and better reliability. The heat needed to raise the temperature of a unit quantity of coating mixture is called specific heat (SH). The electrode will need a lot of

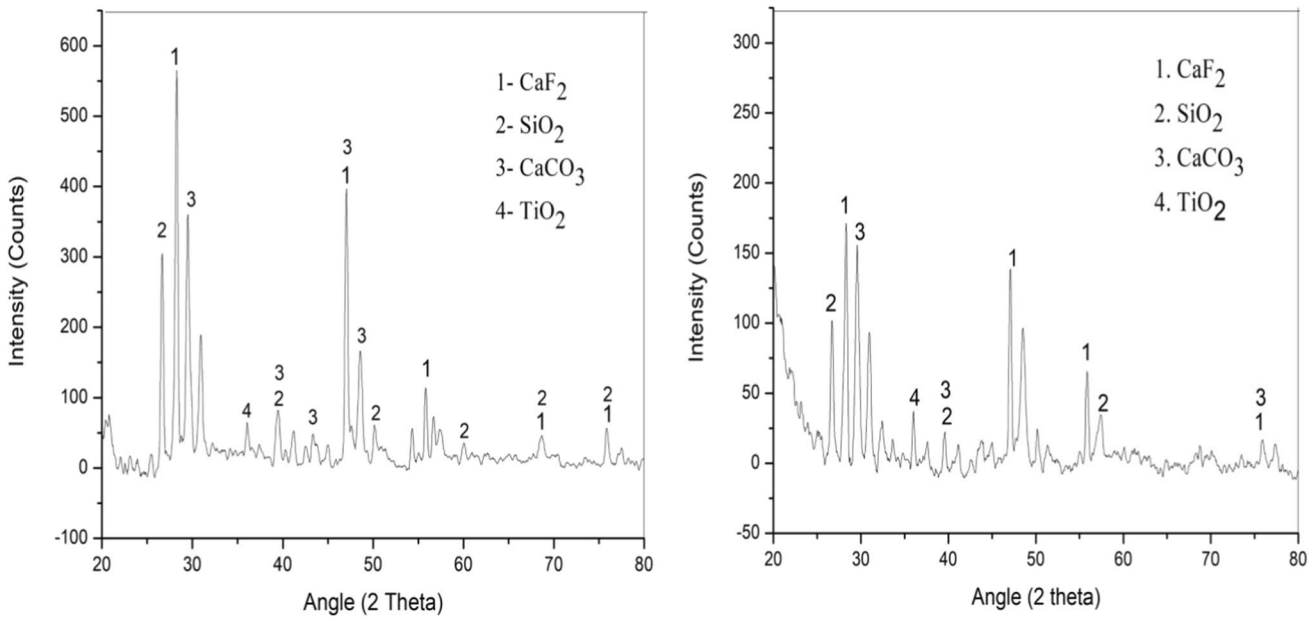

Fig. 7 XRD for coating of 1, and coating 8

energy to melt and fuse; hence the specific heat should be low. Conversely, low specific heat causes the temperature to rise rapidly from modest heat input, causing rapid temperature rise. Hence it causes an exothermic reaction that releases a large amount of heat and damages the weld.

7 Contour Plots

There is variation in the response value by changing the input parameters, which can be seen by Contour plots. The different colors of the contour can achieve the value for the different ranges of particular responses. The crossing lines may also be used to indicate the constant response value variations in the coating composition. Every contour curve shown provides stable value of different properties and every marked point on the graph shows thirteen design points. The contour plot for different properties can be shown in Fig.10.

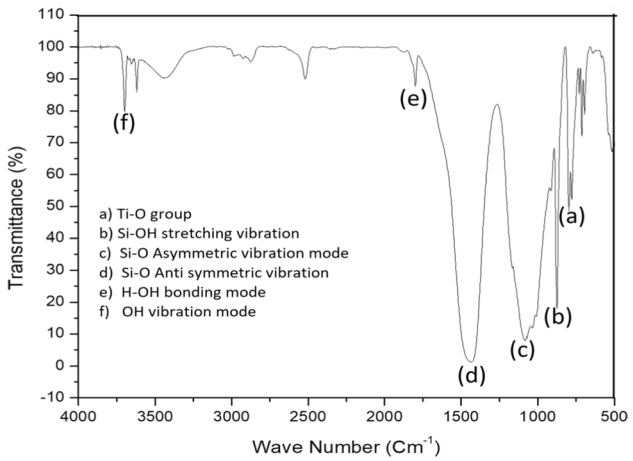

Fig. 8 FTIR curves of the coating composition

8 Model Validation

Randomly selecting three different compositions from the design matrix, the developed regression model was validated with respect to the actual value obtained from the experiment to the predicted value obtained from the developed model. Model validation was done to estimate the concurrency of actual results obtained from the experiment with the developed regression model. Tables 9 and 10 represents the error validation for different thermophysical responses.

9 Conclusions

- A regression model is developed for different properties to analyze each property's effect, individual, binary, and tertiary component interactions.
- X-ray diffraction and Fourier transformation were performed to examine the various phases and structural behavior of different electrode coatings. Si-O and Ti-O symmetric, as well as asymmetric vibration modes, were observed.
- Individual constituents affect density significantly. CaO. CaF_2, $CaO.SiO_2$, and $CaF_2.SiO_2$ is the most effective

Table 7 Regression models for various responses

Property	Source	SS	DF	MSS	F value	P Value	Significance	R^2
Density	Model	0.020	5	4.091E-003	8.15	0.0078	Significant	0.85
	Linear mixture	6.411E-003	2	3.205E-003	6.50	0.0254	Significant	
	CaF_2. CaO	8.785E-003	1	8.785E-003	17.82	0.0039	Significant	
	SiO_2.CaO	1.482E-003	1	1.482E-003	3.01	0.1265	Not-Significant	
	SiO_2.CaF_2	2.636E-003	1	2.636E-003	5.35	0.0540	Not-Significant	
	Residual	3.451E-003	7	4.930E-004				
	Cor Total	0.024	12					
Enthalpy	Model	1.146E+008	5	2.291E+007	4.26	0.0425	Significant	0.75
	Linear mixture	6.168E+007	2	3.084E+007	5.73	0.0336	Significant	
	CaO. CaF_2	1.558E+006	1	1.558E+007	2.89	0.1328	Not-Significant	
	CaO.SiO_2	1.432E+007	1	1.432E+007	2.66	0.1470	Not-Significant	
	CaF_2.SiO_2	2.399E+007	1	2.399E+007	4.46	0.0727	Not-Significant	
	Residual	3.769E+007	7	5.384E+006				
	Cor Total	1.523E+008	12					
Thermal Conductivity	Model	2.899E-003	5	5.685E-004	5.30	0.0248	Significant	0.79
	Linear mixture	1.203E-003	2	6.013E-004	5.61	0.0352	Significant	
	CaF_2. CaO	1.110E-003	1	1.110E-003	10.36	0.0147	Significant	
	SiO_2.CaO	2.022E-005	1	2.022E-005	0.19	0.6771	Not-Significant	
	SiO_2.CaF_2	4.715E-004	1	4.715E-004	4.40	0.0741	Not-Significant	
	Residual	7.503E-004	7	1.071E-004				
	Cor Total	3.593E-003	12					
Thermal Diffusivity	Model	2.325E-003	5	4.651E-004	5.20	0.0260	Significant	0.79
	Linear mixture	2.229E-003	2	1.114E-003	12.47	0.0049	Significant	
	CaO. CaF_2	3.460E-006	1	3.460E-006	0.039	0.8496	Not-Significant	
	SiO_2.CaO	4.008E-005	1	4.008E-005	0.45	0.5246	Not-Significant	
	SiO_2.CaF_2	5.592E-005	1	5.592E-005	0.63	0.4549	Not-Significant	
	Residual	6.257E-004	7	8.938E-005				
	Cor Total	2.951E-003	12					
Specific heat	Model	0.042	5	8.359E-003	4.72	0.0332	Significant	0.77
	Linear mixture	5.515E-003	2	2.757E-003	1.56	0.2759	Not-Significant	
	CaO. CaF_2	0.027	1	0.027	15.09	0.0060	Significant	
	CaO.SiO_2	8.162E-003	1	8.162E-003	4.61	0.0690	Not-Significant	
	CaF_2.SiO_2	7.768E-005	1	7.768E-005	0.044	0.8401	Not-Significant	
	Residual	0.012	7	1.772E-003				
	Cor Total	0.054	12					
Weight Loss	Model	0.24	5	0.048	4.87	0.0306	Significant	0.78
	Linear mixture	0.14	2	0.072	7.30	0.0194	Significant	
	CaO. CaF_2	0.091	1	0.091	9.28	0.0187	Significant	
	CaO.SiO_2	5.697E-003	1	5.697E-003	0.58	0.4711	Not-Significant	
	CaF_2.SiO_2	8.424E-004	1	8.424E-004	0.086	0.7781	Not-Significant	
	Residual	0.069	7	9.819E-003				
	Cor Total	0.31	12					

binary mixture which has an increasing effect on density. The lower value of the variance coefficient specifies the good reliability and precision of the experiment conducted.

- The developed regression model for enthalpy represents a significant p value of 0.0425, and it was observed that binary interaction of $CaO.SiO_2$ and $CaF_2.SiO_2$ is the most effective and has an increasing effect on change in enthalpy.
- The weight loss of coating observed during thermogravimetric analysis is affected by individual constituents significantly. The binary interaction of SiO_2.CaO and CaF_2.

Table 8 Impact of the mineral constituents on the thermophysical and physicochemical properties

Type	Term	Density (D)	Enthalpy (ΔH)	Thermal conductivity (T.C.)	Thermal diffusivity (T.D.)	Specific heat (S.H.)	Weight loss (ΔW)
Individual	CaO	↓	↑	↓	↑	↓	↑
	CaF_2	↓	↑	↓	↓	↓	↑
	SiO_2	↓	↑	↑	↑	↓	↓
Binary	CaF_2.CaO	↑	↓	↑	↑	↑	↓
	SiO_2.CaO	↑	↑	↓	↓	↑	↑
	$CaF_2.SiO_2$	↑	↑	↑	↑	↑	↑

↑ – Increasing effect, ↓ – Decreasing effect

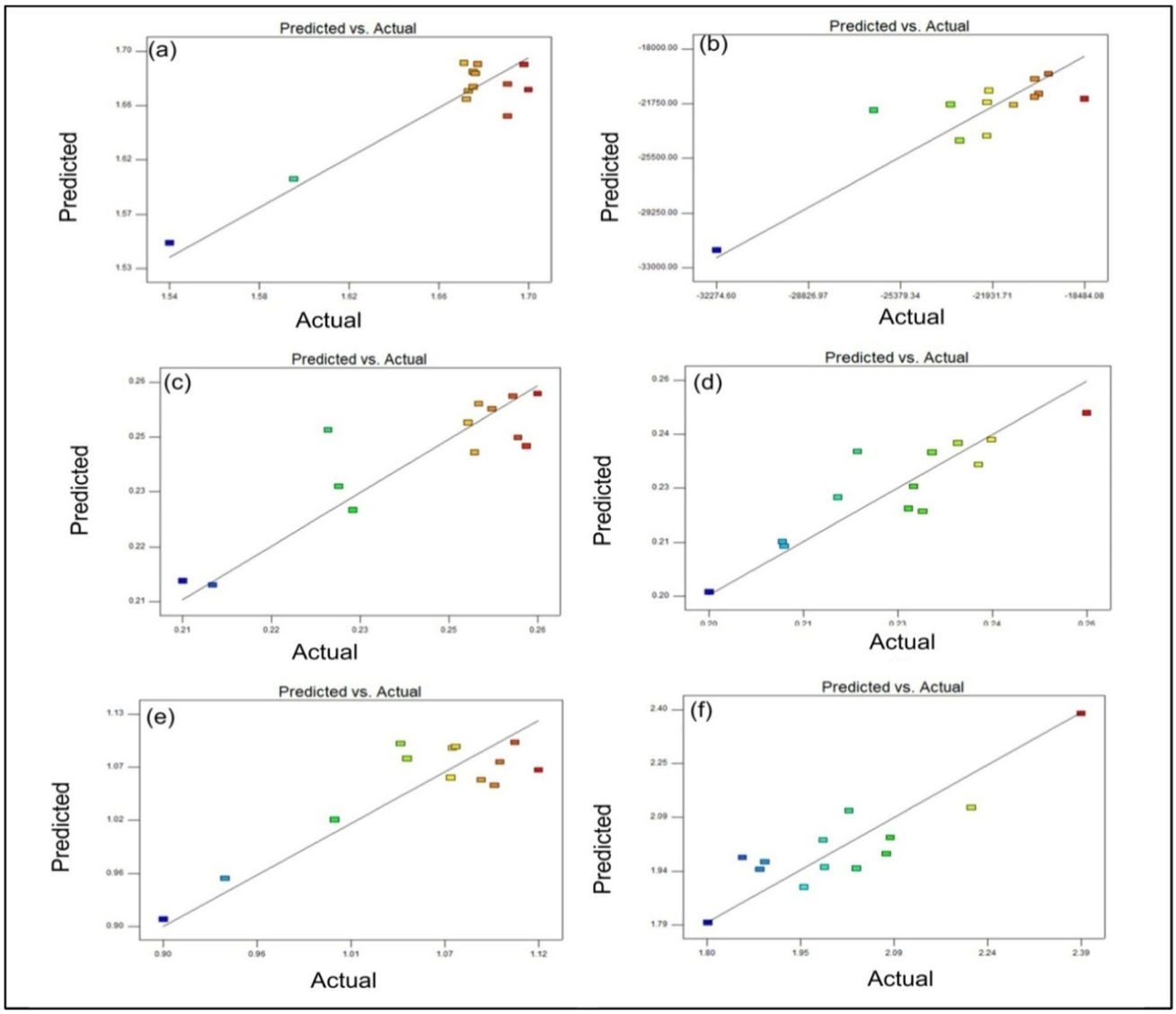

Fig. 9 Predicted versus actual plot: (**a**) D (**b**) ΔH (**c**) T.C. (**d**) T.D.(**e**) S.H.(**f**) ΔW

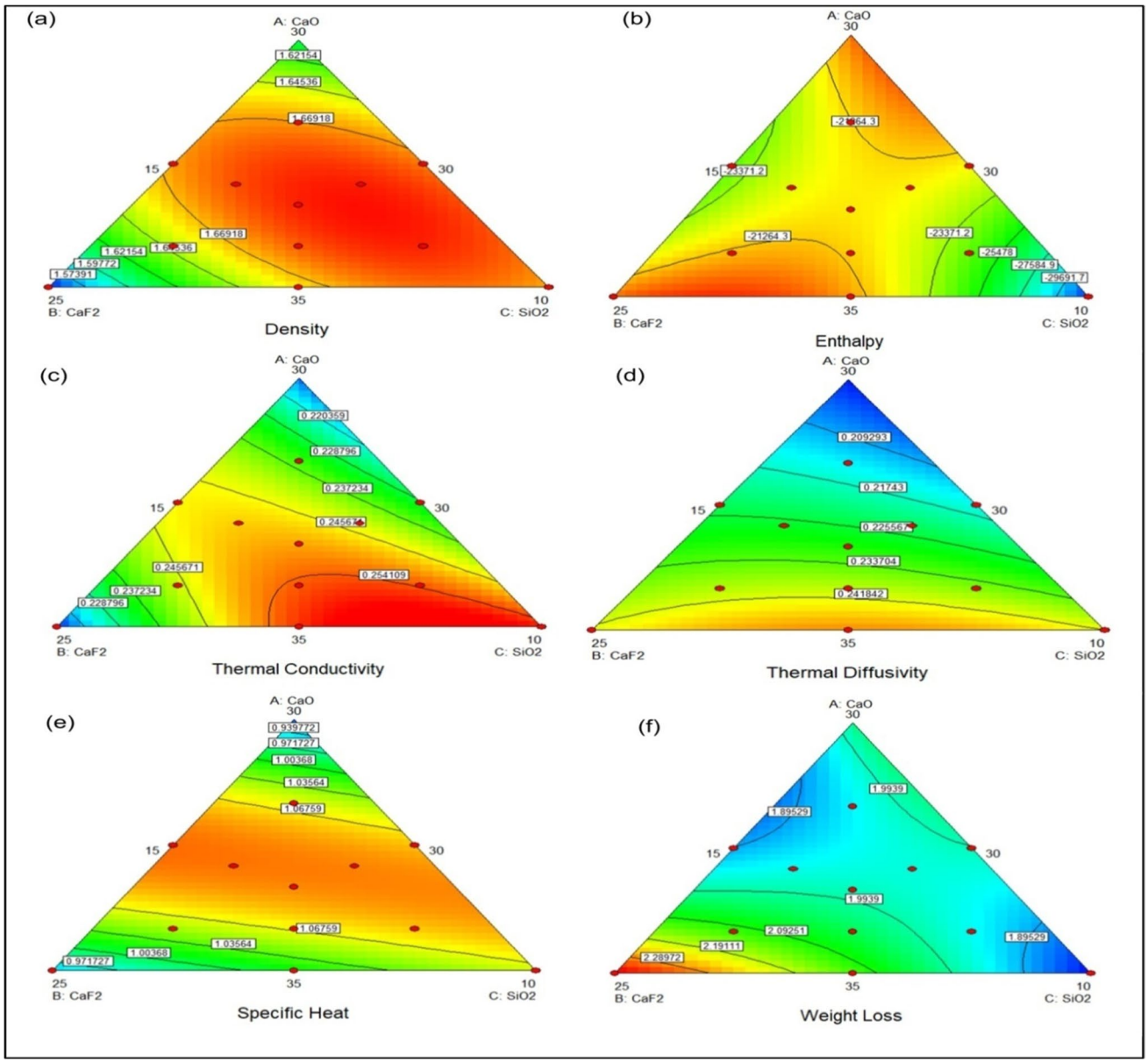

Fig. 10 Surface profiles of various responses

Table 9 Error percentage of different properties:- D, ΔW, and ΔH

Coating			PV			AV			EP		
CaO	CaF_2	SiO_2	ρ	ΔW	ΔH	ρ	ΔW	ΔH	ρ	ΔW	ΔH
30.00	30.00	15.00	1.600	2.029	19,712.47	1.593	1.982	19,829.20	0.439	2.371	0.588
35.00	27.50	12.50	1.662	2.282	20,859.95	1.668	2.218	22,065.60	0.359	2.885	5.463
34.17	26.67	14.17	1.652	2.122	21,082.72	1.686	2.023	20,192.10	2.016	4.893	4.410
							Avg. Error %		**0.938**	**3.383**	**3.487**

SiO_2 is the most favorable and has an increasing effect on weight loss. The lower value of the variance coefficient is (CV = 4.92%), indicating better reliability and precision.

- The thermal properties of coating composition observed during hot disc are affected by individual and binary mixture constituents. Binary mixture CaF_2.CaO and CaF_2.

Table 10 Error percentage of different properties:- T.C, T.D, and S.H

Coating			PV			AV			EP		
CaO	CaF_2	SiO_2	TC	TD	S.H.	TC	TD	S.H.	TC	TD	SH
30.00	30.00	15.00	0.2119	0.2011	0.9082	0.2128	0.2004	0.9002	0.423	0.349	0.888
35.00	27.50	12.50	0.2572	0.2499	1.0157	0.2592	0.2587	1.002	0.771	3.401	1.367
Avg. Error %									**1.95**	**1.87**	**1.96**

D- density, ΔW- weight loss, ΔH- enthalpy, T.C- conductivity, T.D- diffusivity, SH- specific heat, PV- predicted value, AV- actual value, EP- error percentage

SiO_2 is having an increasing effect on thermal conductivity while other components show negative effect on thermal conductivity.

- The developed regression model for thermal diffusivity with a p value of 0.0260 indicates the significance and primary constituents affect the thermal diffusivity significantly. Binary mixture CaF_2.CaO, CaF_2.SiO_2 shows an increasing effect on thermal diffusivity. A lower variance coefficient (4.12%) was shown with this model, indicating good precision and reliability for experimentation.
- The developed model for specific heat having a p value of 0.0332 is significant. Binary mixture constituents CaF_2.CaO, SiO_2.CaO is the most effective and has an increasing effect on specific heat.
- Model validation was done to estimate the concurrency of actual results obtained from the experiment. The average percentage of error is under limits and represents less variation among predicted and actual values.

Acknowledgements It is requested to editorial board to please acknowledge the present research for possible publication in Silicon journal. The content is new and unpublished.

Author Contributions It is certified on behalf of corresponding author (Vijay Kumar) that corresponding authors are contributed in the present manuscript.

Funding It is certified on behalf of corresponding author (Vijay Kumar) that present research is not funded by any external agency.

Data Availability I Vijay Kumar (Corresponding Author) certified that data & material will be available on author's request.

Declarations

Ethical Approval I Vijay Kumar (Corresponding Author) on behalf of other co-authors certified that I have taken the ethical approval to publish the data presented in the manuscript. Also the data used in this manuscript (such as figures) has been cited in this paper.

Consent to Participate NA.

Consent of Publication I Vijay Kumar (Corresponding Author) on behalf of other coauthors certified that I have taken the permission to publish the present content.

Research Involving Human Participants and/or Animals The present research is involved for human participants.

Conflict of Interest It is certified on behalf of corresponding author (Vijay Kumar) that present research is not funded by any external agency and authors declared that there is no conflicts of interest in the present research.

References

1. Pavan AHV, Vikrant KSN, Ravibharath R, Singh K (2015) Development and evaluation of SUS304H-IN 617 welds for advanced ultra super-critical boiler applications. Mater Sci Eng A 642:32–41
2. Shah Hosseini H, Shamanian M, Kermanpur A (2011) Characterization of microstructures and mechanical properties of Inconel 617/310 stainless steel dissimilar welds. Mater Charact 62(4):425–431
3. Dupont JN (2012) Microstructural evolution and high-temperature failure of ferritic to austenitic dissimilar welds. Int Mater Rev 57(4):208–234
4. Fuchs R, Heuser H, Hahn B (2010) Welding of dissimilar materials. Mater High Temp 27(3):183–190
5. Akram J, Kalvala PR, Chalavadi P, Misra M (2018) Dissimilar metal weld joints of P91/Nimicrostructural characterization of HAZ of P91 and stress analysis at the weld interfaces. J Mater Eng Perform 27(8):4115–4128
6. Kumar V, Chhibber R (2022) Experimental investigation on SMAW electrode coatings developed using CaO–SiO_2–CaF_2–SrO based coating system. Ceram Int. https://doi.org/10.1016/j.ceramint.2022.06.187
7. Bhandari D, Chhibber R, Arora N, Mehta R (2019) Investigations on weld metal chemistry and mechanical behaviour of bimetallic welds using CaO-CaF_2-SiO_2-Ni based electrode coatings. Proceedings of the Institution of Mechanical Engineers, Part L, Journal of Materials: Design and Applications 233(4):563–579
8. Mahajan S, Chhibber R (2019) Design and development of shielded metal arc welding (SMAW) electrode coatings using a CaO-CaF_2-SiO_2 and CaO-SiO_2-Al_2O_3 flux system. JOM 71(7):2435–2444
9. Khan WN, Chhibber R (2020) Physicochemical and thermophysical characterization of CaO-CaF_2-SiO_2 and CaO-TiO_2-SiO_2 based electrode coating for offshore welds. Ceram Int 46(7):8601–8614

10. North TH, Bell HB, Nowicki A, Craig I (1978) Slag/metal interaction, oxygen and toughness in submerged arc welding. Weld J (Miami, Fla). 57(3):63–75
11. Mitra U, Eagar TW (1984) Slag metal reactions during submerged arc welding of alloy steels. Metall Trans A, Phys Metall Mater Sci 15 A(1):217–227
12. Bhandari D, Chhibber R, Arora N, Mehta R (2016) Investigation of TiO_2-SiO_2-CaO-CaF_2based electrode coatings on weld metal chemistry and mechanical behaviour of bimetallic welds. J Manuf Process 23:61–74
13. Kumar V, Chhibber R (2022) Physicochemical and thermophysical properties of CaO–TiO_2–SiO_2–Na_3AlF_6 system based electrode coating for AUSC power plant. Ceram Int. https://doi.org/10.1016/j.ceramint.2022.03.005
14. Khan WN, Chhibber R (2021) Investigations on the effect of CaO-CaF_2-TiO_2-SiO_2 based electrode coating constituents and their interactions on weld chemistry. Ceram Int 47(9):12483–12493
15. Jindal S, Chhibber R, Mehta NP (2013) Investigation on flux design for submerged arc welding of high-strength low-alloy steel. Proc Inst Mech Eng Part B J Eng Manuf 227(3):383–395
16. Sharma L, Chhibber R (2019) Design and development of submerged arc welding fluxes using TiO_2-SiO_2-CaO and SiO_2-CaO-Al_2O_3 flux system. Proc Inst Mech Eng Part E J Process Mech Eng 233(4):739–762
17. Natalie CA, Olson DL (1986) Physical and chemical behaviour of welding fluxes. Ann RevMaterialScience:389–413
18. Mitra U, Eagar TW (1991) Slag-metal reactions during welding: part III. Verification of the theory. Metall Trans B 22(1):83–100
19. Qin R, He G (2013) Mass transfer of nickel-base alloy covered electrode during shielded metal arc welding. Metall Mater Trans A Phys Metall Mater Sci 44(3):1475–1484
20. Eriksson G, Pelton AD (1993) Critical evaluation and optimization of the thermodynamic properties and phase diagrams of the CaO-Al_2O_3, Al_2O_3-SiO_2, and CaO-Al_2O_3-SiO_2 systems. Metal Trans B 24(5):807–816
21. Wang H, Qin R, He G (2016) SiO_2 and CaF_2 behavior during shielded metal arc welding and their effect on slag detachability of the CaO-CaF_2-SiO_2 type ENiCrFe-7-covered electrode. Metall Mater Trans A Phys Metall Mater Sci. 47(9):4530–4542
22. Burck PA, Indacochea JE, Olson DL (1990) Effects of welding flux additions on 4340 steel weld metal composition. Weld J (Miami, Fla) 69(3)
23. Mills KC, Su Y, Fox AB, Li Z, Thackray RP, Tsai HT (2005) A review of slag splashing. ISIJ Int 45(5):619–633
24. Sham K, Liu S (2014) Flux-coating development for SMAW consumable electrode of high-nickel alloys. Weld J 93(8):271s–281s
25. Elaiyarasan U, Kumar VS, Senthilkumar C (2021) Effect of parameters on microstructure of electrical discharge coated ZE41A magnesium alloy with tungsten carbide-copper composite electrode. Surf Topogr: Metrol Prop 9:025006. https://doi.org/10.1088/2051-672X/abf326
26. Elaiyarasan U, Vinod B, Nallathambi K Response surface methodology study on electrical discharge deposition of AZ31B magnesium alloy with powder composite electrode, Int J Interact Des Manuf, https://doi.org/10.1007/s12008-022-00923-z
27. Ananthi N, Elaiyarasan U, Satheeshkumar V, Senthilkumar C, Sathiyamurthy S. Effect of wc–cu composite electrodes on material deposition rate, microhardness and microstructure of electrical discharge coated magnesium alloy, https://doi.org/10.1142/S0218625X22500500
28. Mahajan S, Chhibber R (2020) Investigation on slags of CaO-CaF_2-SiO_2-Al_2O_3 based electrode coatings developed for power plant welds. Ceram Int 46(7):8774–8786
29. Sharma L, Chhibber R (2019) Design of TiO_2-SiO_2-MgO and SiO_2-MgO-Al_2O_3-based submerged arc fluxes for a multipass bead on plate pipeline steel welds. Journal of Pressure Vessel Technology, Transactions of the ASME 141(4)
30. Sharma L, Chhibber R (2019) Investigating the physicochemical and thermophysical properties of submerged arc welding fluxes designed using TiO_2-SiO_2-MgO and SiO_2-MgO-Al_2O_3 flux systems for linepipe steels. Ceram Int 45(2):1569–1587
31. Kumar V, Kumar J, Chhibber R, Sharma L (2022) Experimental study on wettability at high-temperature using TiO_2-SiO_2-CaO-Na_3AlF_6 based electrode coating for AUSC thermal power plant. Silicon. https://doi.org/10.1007/s12633-022-01824-2
32. McLean RA, Anderson VL (1966) Extreme vertices design of mixture experiments. Technometrics 8(3):447–454
33. Mukerji J (1965) Phase Equilibrium Diagram CaO-CaF_2-2CaO. SiO_2. J Am Ceram Soc 48(4):210–213
34. Garai M, Sasmal N, Molla AR, Karmakar B (2015) Structural effects of Zn+2/mg+2 ratios on crystallization characteristics and microstructure of fluorophlogopite mica-containing glass-ceramics. Solid State Sci 44:10–21
35. Kaur G, Kumar M, Arora A, Pandey OP, Singh K (2011) Influence of Y_2O_3 on structural and optical properties of SiO_2-BaO-ZnO-xB_2O_3-(10-x) Y_2O_3 glasses and glass ceramics. J Non-Cryst Solids 357(3):858–863
36. Sowmya T, Sankaranarayanan SR (2004) Spectroscopic analysis of slags- preliminaryobservations. VII Int Conf on Molten Slags Fluxes and Salts, The South African Institute of Mining and Metallurgy
37. Garai M, Sasmal N, Molla AR, Singh SP, Tarafder A, Karmakar B (2014) Effects of nucleating agents on crystallization and microstructure of fluorophlogopite mica-containing glass-ceramics. J Mater Sci 49(4):1612–1623
38. Kerstan M, Muller M, Russel C (2011) Binary, ternary and quaternary silicates of CaO, BaO and ZnO in high thermal expansion seals for solid oxide fuel cells studied by high-temperature X-ray diffraction (HT-XRD). Mater Res Bull 46(12):2456–2463